Probabilistic seismic vulnerability assessment of aluminium alloy reticulated shells with consideration of uncertainty

Zhiwei Yu[a], Chen Lu[b,*], Huihuan Ma[c], Fan Kong[d]

[a] School of Civil Engineering, Guangzhou University, Guangzhou, China
[b] School of Business Administration, Guangzhou University, Guangzhou, China
[c] School of Civil Engineering, Sun Yat-Sen University, Guangzhou, China
[d] School of Civil Engineering and Architecture, Wuhan University of Technology, Wuhan, China

ARTICLE INFO

ABSTRACT

Single-layer aluminium alloy cylindrical shells are established using the powerful finite element (FE) software package ABAQUS. Furthermore, the probability distribution models of different random parameters in structural modelling are summarized. Forty seismic ground motion records are selected to consider the uncertainty of earthquakes. Sensitivity analysis of modelling parameters is conducted to determine the parameters with the greatest influence on seismic responses. The incremental dynamic analysis (IDA) method is performed on aluminium alloy cylindrical latticed shell structures with different structural parameters. After applying the damage index and structural performance levels of the latticed shells proposed in this paper, the probabilistic seismic demand model and probabilistic seismic capacity model are established. The seismic performance and the collapse capacity of different aluminium alloy cylindrical latticed shells are discussed based on the FE results. Furthermore, vulnerability curves are obtained according to the IDA results, which can be utilized to predict the failure probability and to evaluate the structural performance of aluminium alloy cylindrical latticed shells under different levels of earthquakes.

1. Introduction

Aluminium alloys have become a widely applied construction material in transportation applications in the aviation, aerospace, automobile, mechanical manufacturing, shipbuilding and chemical industries [1]. In recent years, they have developed into an important substitute of structural steel, especially for light structures, such as long-span spatial structures, tower structures and bridges [2]. The increase of aluminium alloys in spatial structures, such as reticulated shells, is a result of their superior characteristics to structural steel, such as their low density, high strength-to-weight ratio, low maintenance costs and good recyclability. These alloys also provide comparable ease of manufacturing and superior aesthetics. Many representative aluminium reticulated spatial structures have been established in the United States, Europe and China [3–4]. Most aluminium reticulated spatial structures are single-layer reticulated shells. Due to their importance and specialty to building functions, once the reticulated shells are damaged or collapse, a large direct or indirect economic loss or casualty results. However, the Chinese seismic code only aims to achieve the performance level of life safety, which is not capable of satisfying users'

needs. The analysis of the seismic fragility of aluminium reticulated shells both provides theoretical support to the performance-based seismic design and lays the foundation for the evaluation of seismic loss.

Compared with the work on steel latticed shells, that on aluminium alloy latticed shells is still in the developing stage. Research has also been carried out on the elasto-plastic stability, dynamic behaviour and failure mechanism of aluminium alloy shell structures [5–11]. Xiong zhe [5] investigated the elasto-plastic stability of single-layer latticed shells with aluminium alloy gusset joints and found the semi-rigid performance of the AAG connections to greatly influence the buckling characteristic of Kiewitt shells. Ishikawa [6–9] analysed the behaviour of a double-layer aluminium alloy lattice gridded roof under different loads. Hiyama Yujiro [9] investigated the global buckling behaviours of an aluminium alloy double-layer spatial latticed structure with tubular pipes, ball connections and joining bolts via experimentation and analysis. Xie Zhihong [10] studied the natural vibration characteristics of an aluminium alloy double-layer reticulated shell with various structural dimensions and analyzed the seismic time-history responses using the Newmark integral method. Guo [11] tested aluminium alloy

---

members under a compressive load.

Aluminium alloy is characterized by prominent limited ductility and strain hardening. However, steel has the assumption of perfect plasticity and unlimited ductility. In the actual design of structures, 6000 series aluminium alloys have been widely utilised due to their favourable performance combinations [12]. Of the 6000 series aluminium alloys, the 6082 aluminium alloy is one of the most recent and is prevalent and widely used in Europe and America [13]. The 6082 aluminium alloy possesses high-quality structural behaviours, such as favourable corrosion resistance, high strength-to-weight ratio, good mechanical behaviour and good weldability [14]. Therefore, due to the limited research on large-span aluminium alloy (6082) latticed shells, this paper focuses on probabilistic seismic vulnerability assessment. The analytical model of a single-layer aluminium alloy cylindrical shell is established using the finite element (FE) software ABAQUS. The probability distribution models of the different random parameters in structural modelling are summarized. Historical earthquake records are chosen from the Next Generation Attenuation Models ground motion database of the Pacific Earthquake Engineering Research (PEER) Center to describe the uncertainty of earthquakes. The incremental dynamic analysis (IDA) method is performed on aluminium alloy cylindrical latticed shell structures with different structural parameters. After applying the damage index and structural performance levels of the reticulated shells proposed, the probabilistic seismic demand model (PSDM) and the probabilistic seismic capacity model (PSCM) are set up according to the IDA data and the fragility curves are obtained. In addition, the seismic performance and collapse capacity of different aluminium alloy cylindrical reticulated shells are discussed based on the FE results.

2. Analysis modelling

2.1. Analysis model

A single-layer aluminium alloy cylindrical latticed shell is one of the typical spatial structures modelled by the FE software ABAQUS, as illustrated in Fig. 1. The length of the analytical model (L) is 36 m, the width (B) is 20 m and tubular pipes are selected as the members of the analytical model. The sizes of the tubular members of the cylindrical shells are designed according to the static stability analysis. Element B31 in ABAQUS is adapted to simulate the tubular pipes of the cylindrical latticed shell. The Beam31 element has eight integration dots on the cross-section, as illustrated in Fig. 2. When the members are damaged, there are different degrees of yielding development on the cross-section (1P ~ 8P, as illustrated in Fig. 2). The symbol nP represents n yielded integration dots on the cross-section and 8P represents that the whole section yielded. The percentage of the 1P ~ 8P pipes indicates the scope in the degree of the yielded members of the single-layer cylindrical shell composed of aluminium alloy. The numbering of the FE models for the shells is shown in Fig. 3.
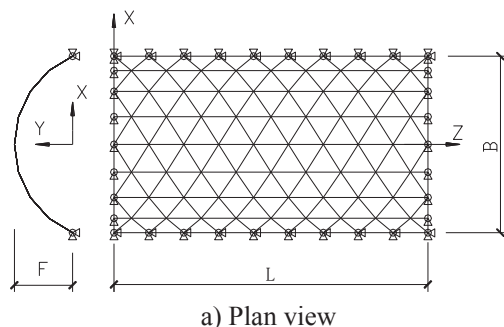
2.2. Material properties

The behaviours of aluminium alloy are examined via an experiment [1,15], in which 45 specimens of 6082-T6 aluminium alloy, including 15 circle pipe specimens, 15H-section specimens and 15 rectangular hollow section specimens, are tested.

For the 'round-house' type stress–strain curves of materials, including aluminium and stainless alloys, the constitutive model is established by the Ramberg-Osgood expression, shown as the canonical Eq. (1) [16]:

$$\varepsilon = \frac{\sigma}{E} + 0.002\left(\frac{\sigma}{\sigma_{0.2}}\right)^m \tag{1}$$

where E is Young's modulus, $\sigma_{0.2}$* MERGEFORMAT is the static 0.2% proof stress and m indicates the level of strain hardening. Although deformation is the primary focus, m can be computed using $m = \ln 2/\ln(\sigma_{0.2}/\sigma_{0.1})$* MERGEFORMAT, in which $\sigma_{0.1}$* MERGEFORMAT is the 0.1% proof stress.(see Fig. 4)

3. Sensitivity study of modelling parameters

The sources of uncertainty that influence structural behaviour can be characterized as aleatory and epistemic in nature [17]. Many parameters of the analytical model can be ascribed a lack of knowledge of the actual model parameters. However, other parameters can be derived from aleatory uncertainty, including the inherent variability in a material's behaviours (e.g., aluminium alloy strength). The origins of uncertainty are presented in the modelling and behaviour evaluation of single-layer aluminium alloy cylindrical shells. The most common uncertainties are the mechanical characteristics of the material, the loads, viscous damping and the dimensions of the members and others. Basically, it is possible to include all types of epistemic uncertainties, which can be described by means of random variables. However, it is practical to consider only a limited number of the random variables, only those that have a significant influence on the seismic response of the structure, in order to reduce the size of the set of structural models, usually referred to by the number of simulations. Probabilistic Model Code [18] illustrated the uncertainty parameters for most types of the structures. So far there are few statistics results for aluminum structures. Thus, due to the absence of statistics data, the uncertainty parameters can be selected as the reference of other metal structures. According to Probabilistic Model Code [18] and reference [1], this paper selected 11 uncertainty parameters and seismic uncertainty for the aluminum structures including mechanical characteristics of the material, the loads, viscous damping and the modelling of the structure, which can cover most of the influential uncertainty.

3.1. Structural geometry model

The uncertainty of a structure is mainly represented by the randomness in the parameters of structural modelling. For reticulated shell

a) Plan view   b) 3D view
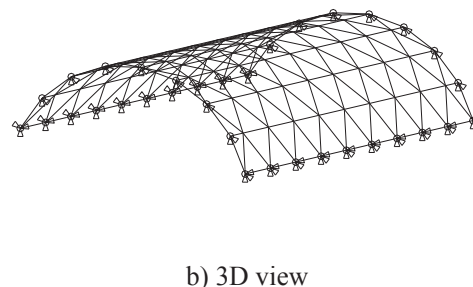
Fig. 1. Three-way, gridded, single-layer, cylindrical shell composed of aluminium alloy.
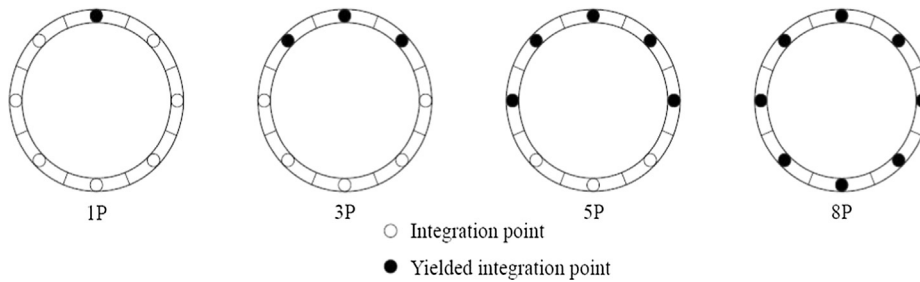
Fig. 2. Definition of diverse degrees of plastic development for the cross-section of the B31 element.
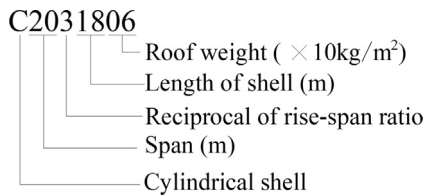
Fig. 3. Numbering of the FE models for the shells.

structures, the modelling parameters can be divided into four categories: material property parameters, structural dynamic characteristics parameters, loading parameters and the geometric parameters of the members.

3.1.1. Material property parameters

The material property parameters mainly include the static 0.2% proof stress $\sigma_{0.2}$* MERGEFORMAT, the elastic modulus E, the degree of strain hardening n and Poisson's ratio v* MERGEFORMAT. The mean value of $\sigma_{0.2}$* MERGEFORMAT is 272.22 MPa with a COV of 0.14, which obeys a normal distribution [18]. The mean value of E is 70,233 MPa with a COV of 0.05, which obeys a lognormal distribution. The mean value of n is 25.24 with a COV of 0.27, which obeys a normal distribution. The mean value of v* MERGEFORMAT is 0.35 with a COV of 0.06, which obeys a lognormal distribution according to the recommendation of the JCSS.

3.1.2. Structural dynamic characteristics parameters

Damping is one of the dynamic characteristic parameters of structures. It is especially important for the dynamic response analysis of long-span and high-rise structures. Structural damping is usually divided into two categories: hysteretic damping and viscous damping. This paper considers the randomness of viscous damping, which is assumed to apply to Rayleigh damping theory. The value of the damping ratio should be obtained by statistical analysis based on the measured and experimental results of the structures. Some experimental data on the variability in viscous damping ratio are available. In this paper, all the input random variables considered for the determination of the set of structural models were assumed to be uncorrelated. Reference [19] presents the results of system identification for different structures including steel structures and reinforced concrete structures. It shows that the damping ratio appears to be modestly sensitive to shaking intensity. Analysis of the data suggests a coefficient of variation on damping ratio of approximately 0.3 ∼ 0.4. The proposed approach [20] combines IDA analysis and the latin hypercube sampling (LHS) technique, which is used to define a set of structural models. These models reflect the epistemic uncertainty. The statistical characteristics of random variables are also presented in Reference [20]. A normal distribution was assumed for viscous damping ratio with coefficient of variation 0.4. According to references [18–20], a normal distribution was assumed for viscous damping ratio with the mean value of 0.02 and CV of 0.4 in this paper. The negative damping ratio will lead to an increasing dynamic response until it is infinite. No convergent solution can be obtained in finite element simulation. Therefore, the truncated normal distribution

is assumed actually for damping ratio in the analysis in order to keep the the values of damping ratio positive. The responses of the reticulated shells under seismic loadings can be obtained in the incremental dynamic analysis.

3.1.3. Loading parameters

Dead and live loads are two important loading parameters in the design of reticulated shells. When determining the cross-sections of the reticulated shell members, the load value is taken as the sum of the standard values of the dead and live loads. In this paper, the standard value of the dead loads of light, medium and heavy roof loads are 40, 100 and 160 kg/m² respectively, which obey normal distributions with a COV of 0.07. The standard value of the live load is 50 kg/m², which obeys an extreme value distribution (type I) with a COV of 0.229.

3.1.4. Geometric parameters of members

The geometric parameters of the members considered in this paper include the diameter (D), the wall thickness (t), the deviation of the joints and the initial bending of the member. The pipe dimensions of latticed shells can be obtained from static analysis. The mean value of the member sections is assumed to be the design value (shown in Table 1) and the COV is 0.02. For node deviations, it is suggested that the deviations of individual nodes obey a normal distribution with a mean value of 0 and a variance of $L/2,000$[21]. The initial bending of a member can be defined by two variables: the initial bending angle and amplitude. It is suggested that the initial bending angle of the member be uniformly distributed in the interval [0, 360) and that the initial bending amplitude of the member obeys an extreme value distribution (type I), as shown in Eqs (2) to (4)[22]:

$$F(\delta) = 1 - \exp\{-\exp[-v(\delta - q)]\} \tag{2}$$

$$v = \frac{5.9}{(l/1000)} \tag{3}$$

$$q = \frac{l}{1280} \tag{4}$$

where l is the length of the member, q is the mode of distribution and v* MERGEFORMAT is the measure of skewness.

Overall, 11 structural uncertainties are considered in this paper. Their probability distributions are shown in Table 1.

3.2. Seismic uncertainty model

Seismic uncertainty is represented by the variability of ground motion records caused by many factors, such as the focal mechanism, moment magnitude, epicentral distance and site conditions. In this paper, historical seismic records are selected from the earthquake database to describe the uncertainty of earthquakes.

Forty far-fault ground motion records are chosen from PEER's Next Generation Attenuation Models ground motion database. This ground motion database contains 3,551 earthquake records from 173 earthquakes in California, Japan, Taiwan and other regions with high seismic activity. The principles of selecting earthquake records are as follows:

a) Maximum nodal displacement

b) Ratios of yielding members with *1P*

c) Ratios of yielding members with *8P*
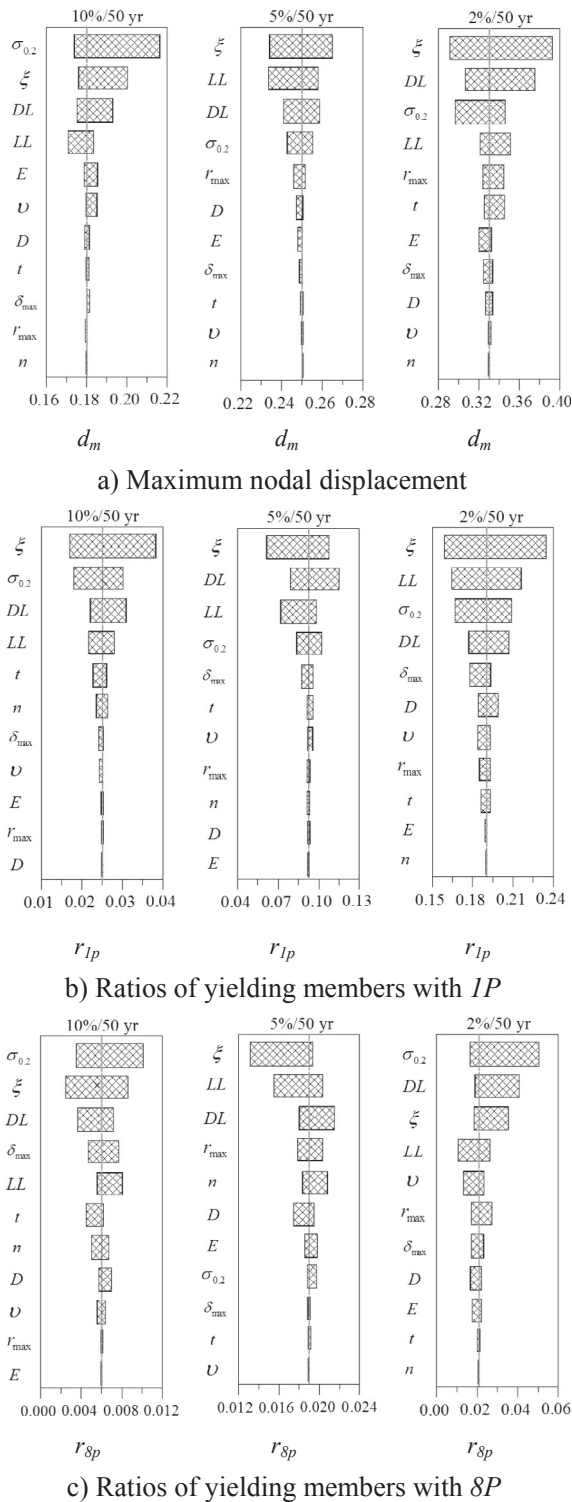
Fig. 4. Tornado diagrams of different response parameters under three hazard levels.

(i) The value of the moment magnitude M_W is between 5.8 and 7.8.
(ii) The epicentral distance R is between 10 km and 60 km.
(iii) The focal depth is less than 20 km.
(iv) The shear wave velocity V_s is greater than 180 m/s^2.
(v) The ground motion record quality has a minimum frequency less than 0.25 Hz.
(vi) Each seismic record must contain three directional components.

In order to consider the randomness of seismic actions, these earthquake records covered different magnitudes, different epicentral distances, different site conditions, different focal mechanisms and different intensities with the specific description as shown in Appendix A. The value of the moment magnitude M_W is between 5.8 and 7.8 in order to exclude the earthquake records with too small or too large magnitude. The shear wave velocity V_s is greater than 180 m/s^2. The site classification is corresponding to class C and D of FEMA450, respectively. In this paper, The PGA is selected to be the index of earthquake ground motion intensity. A more specific description about the earthquakes has been made in the paper. The seismic fortification level refers to the magnitude of earthquake intensity that may be exerted on structures in the future. The seismic fortification level has a direct impact on the seismic performance of structures. There are three seismic levels in Code for seismic design of buildings of China (GB50011-2010) as follows. The first level(frequent earthquakes): when the structures are affected by frequent earthquakes that are less than the seismic fortification intensity in the region, they are generally not damaged or need no repair to continue to use. The second level: when the structures are affected by the seismic fortification intensity equivalent to that of the region, structures may be damaged and can be used after general repair or no repair. The third level(rarely occurred earthquake): When the structures are affected by the rarely occurred earthquake from the prediction of seismic fortification intensity in the region, the structures will not collapse or suffer serious damage. Three seismic levels are considered in this paper. Therefore, the vulnerability analysis of different levels of structural damage can predict the failure probability and evaluate the structural performance of aluminium alloy cylindrical latticed shells under different earthquake levels.

The PGA is the index of earthquake ground motion intensity. In the Increment Dynamic Analysis(IDA), the PGA was gradually increased from 0.1 g. When the latticed shell is in the elastic stage, the scaling factor remains to be 0.1 g. When the latticed shell is in the plastic stage, the scaling factor will change to 0.05 g. For each load amplitude, finite element package ABAQUS is utilized to perform a nonlinear dynamic time-history analysis. And the Fortran program is designed to record different characteristic responses with respect to different seismic load amplitudes. From the variation of the typical characteristic responses, the failure behaviors can be distinguished as well by the comprehensive research on the relation between the characteristic response and the seismic load amplitude.

3.3. Sensitivity analysis

Sensitivity analysis is mainly used to investigate the local influence of a single uncertain factor on the response output of the model. In the analysis, the single input variable of the model can be changed by adding or reducing one standard deviation on the basis of its central value. Other variables remain unchanged by their respective central values. The sensitivity analysis results can be expressed as the variance ratio of output variables relative to each input variable. According to the order of output variation from large to small, the results of each analysis are drawn in the same figure from top to bottom in order to obtain an intuitive tornado diagrams. The detailed analytical procedure is as below:

(1) 11 random variables in Table 1 are selected as their respective median x_{im}, and the finite element models of reticulated shells are established based on x_{im}. The time history analysis under 40 earthquake motions in Appendix A is carried out to obtain the median values of structural response parameters (maximum displacement d_m, yield ratio r_{1p}, r_{3p}, r_{5p} and r_{8p})
(2) Change the value of a single variable step by step while keeping the median x_{im} constant for other variables. Firstly, set the value of the ith variable to be analyzed to 16% tantile which can be expressed as x_{im}-a_i and keep the median values of other variables unchanged.

Table 1
Uncertainty parameters in structural modelling.

Random parameters (unit)	Probability distribution	Mean value	COV
Proof stress $\sigma_{0.2}$* MERGEFORMAT (Mpa)	Normal distribution	272.22	0.14
Elastic modulus E (Mpa)	Lognormal distribution	70,233	0.05
Degree of strain hardening n (-)	Normal distribution	25.24	0.27
Poisson's ratio υ* MERGEFORMAT (-)	Lognormal distribution	0.35	0.06
Viscous damping ratio ξ* MERGEFORMAT (-)	Normal distribution	0.02	0.4
Dead load DL (kg/m^2)	Normal distribution	148.56	0.07
Live load LL (kg/m^2)	Extreme value distribution(1)	30.45	0.229
Diameter of the member D (m)	Normal distribution	0.140	0.02
Wall thickness t (m)	Normal distribution	0.005	0.02
Deviation of joints r_{max} (m)	Extreme value distribution(1)	0.0784	0.0102
Initial bending of the member δ_{max}* MERGEFORMAT (m)	Uniform distribution	0.005*l	0.5668

The median value y_{i16} of the structural response parameters can be obtained by step (1). Then, the value of the ith variable is set to be 84% tantile which is $x_{im} + a_i$ and keep the median values of other variables unchanged. The median value y_{i84} of the structural response parameters can be obtained by step (1).

(3) The median values of structural response parameters in steps (1) and (2) are plotted from top to bottom in the order of corresponding variation ($|y_{i84}-y_{i16}|$). The tornado diagrams of sensitivity of different random parameters to the seismic response parameters can be obtained.

Based on the sensitivity analyses of the 11 structural parameters, three seismic risk levels are considered, in which the exceedance probabilities of 10%, 5% and 2% in 50 years have a corresponding recurrence interval of 475, 975 and 2475 years. Seismic hazard curve of the intensity i can be calculated by the Eqs. (5) and (6) [23]:

$$P(I \geqslant i) = 1 - \exp\left\{ -\left(\frac{\omega - i}{\omega - I_0}\right)^k / 10^{0.9773} \right\}$$

(5)

$$A_{max} = 10^{(i \lg 2 - 0.1047575)}$$

(6)

where, P is exceedance probability; ω* MERGEFORMAT is the upper limit of the seismic intensity, which is usually 12; The coefficient k is defined as shape factor of the intensity probability distribution curve and is used as a characteristic parameter to describe the seismic hazard differences for different areas, which is 9.7932, 8.3339, 6.8713 and 5.4028 when the corresponding earthquake magnitude is 6, 7, 8 and 9, respectively. I_0 is the basic intensity for a 10% exceedance probability in 50 years. A_{max} is the intensity parameter of ground motion (PGA).

The tornado diagrams of different random parameters under three different hazard levels can be obtained by the sensitivity analysis. Fig. 4 shows the tornado diagrams of different structural responses under three different hazard levels and indicates that the proof stress $\sigma_{0.2}$* MERGEFORMAT, the viscous damping ratio ξ* MERGEFORMAT, the dead load DL and live load LL are the top four most influential structural parameters that largely affect structural dynamic responses. The other six parameters have comparatively less influence on structural seismic responses.

4. Probabilistic seismic demand analysis

Probabilistic seismic demand analysis (PSDA) is one of the core contents of the seismic vulnerability analysis. The aim is to establish the PSDM of the structure, which reflects the influence of seismic and structural uncertainty on the dispersion of structural responses.

In this paper, the IDA method is used to carry out the PSDA and to set up the seismic vulnerability curves of reticulated shell structures. The seismic demand placed on various critical components is evaluated according to the establishment of the PSDM. The cloud chart method is utilized to conduct the regression study of the IDA outcomes to obtain the PSDM.

4.1. Damage index

How to define and quantify structural damage under earthquakes is the first significant step in fragility analysis. A damage measure should indicate the systematic destroyed levels of a structure subjected to seismic loads. Damage measures have been proposed for different structures subjected to earthquake loading. Several researchers have proposed a displacement-based method, such as the maximum roof drift ratio, to quantify structural damage [24]. Others have applied an energy-based method that relates the magnitude of hysteretic energy to the degree of damage [25]. Finally, some research has combined the two methods and derived hybrid measures [26]. Yet, these measures are not applicable to reticulated shell structures, which have different dynamic characteristics from other structures.

According to the incremental dynamic analysis on the aluminum reticulated shells, the failure modes of aluminum reticulated shells under earthquakes can be classified into two categories: one is dynamic instability, which exhibits less development of plastic deformation and collapses more abruptly. The structural responses are almost linear behavior, and the structural total stiffness does not change before the collapse, which indicates the structural collapse is mainly caused by the geometric nonlinear effect with obvious dynamic instability characteristics. The other is dynamic strength failure, which displays extensive development of plastic deformation and large displacement before collapse. The structural failure is caused by strong material nonlinearity. It is necessary to consider the damage accumulation of the structure under the earthquakes. Therefore, the damage index D_s can be established to determine the limit states of the aluminum reticulated shells.

In the IDA method, the damage level of a structure can be defined via the intense research on the relation between structural performances and the loading amplitudes of ground motions. In this paper, a new damage index D_s is proposed [27] to describe structural damage levels, which can be estimated using Eq. (7):

$$D_s = c \times \sqrt{(f/L) \cdot (c_1 \cdot p_1^2 + c_2 \cdot p_2^2 + c_3 \cdot p_3^2 + c_4 \cdot p_4^2)}$$

(7)

where p_1, p_2, p_3 and p_4 are the characteristic performances of latticed shells at the damage level and c, c_1, c_2, c_3 and c_4 are constant factors.

Finite element package ABAQUS is utilized to perform a nonlinear dynamic time-history analysis for each load amplitude. And the Fortran program is designed to record different characteristic performances. The characteristic responses of single-layer latticed shells including the maximum nodal displacement of the latticed shell, the ratio of the yielded members and the plastic strain are explained below:

The maximum nodal displacement of lattice shells: the maximum value of the structural displacement with respect to the seismic load amplitude throughout the IDAs.

The ratio (percentage) of yielded pipe members: there are 8 integral points on the cross-section of the beam member. The symbol nP represents that there are n integral points on the cross-section yielded. Ratios of $1P \sim 8P$ members illustrate level of the plastic deformation of the steel structure.

The curves of the characteristic responses with respect to the corresponding seismic load intensity will be recorded as the response curves which will visually illustrate the variation of the characteristic response with the increase of the seismic load amplitude.

The damage index D_s for single-layer cylindrical latticed shells is expressed by Eq. (8):

$$D_S = 0.80 \times \sqrt{100 \times \left(\left(\frac{d_m - d_e}{R \times L}\right)^2 + \left(\frac{\varepsilon_a}{R \times \varepsilon_u}\right)^2\right) + r_1^2 + r_8^2} \tag{8}$$

where L represents the span and R represents the length-width ratio of the cylindrical latticed shell; d_m represents the maximum nodal displacement; d_e represents the nodal displacement when plasticity occurs in the material; ε_a represents the mean strain of the cylindrical latticed shell; ε_u represents the ultimate strain of the aluminium alloy under axial tension; and r_1 and r_8 represent the percentages of $1P$ and $8P$, respectively.

The value of D_s at the limit state of failure is calculated using the damage model, as shown in Fig. 5. As can be seen from Fig. 5, most of the values of D_s corresponding to the limit state are close to 1.0, which indicates that the structural damage model has a good precision and can be used for accurate quantification of limit state of failure for the aluminum reticulated shells.

4.2. Probabilistic seismic demand model

Structural seismic demand D is ordinarily assumed to obey a log-normal distribution [28–30]. The median value of D has an exponential relationship with the seismic intensity IM given in Eq. (9):

$$\mu_{D|IM} = \beta_0 + \beta_1 \ln IM \tag{9}$$

where $\beta_0 = \ln a$ and $\beta_1 = b$ are unknown regression factors. The PSDM is given in Eq. (10):

$$P[D \geqslant d|IM = im] = 1 - \Phi\left[\frac{\ln d - \ln \mu_{D|IM}}{\sigma_{D|IM}}\right] \tag{10}$$

where $\Phi(\cdot)$ is the cumulative probability distribution function of the standardised normal distribution and $\sigma_{D|IM}$ is the logarithmic standard deviation derived from the linear regression of the IDA results given in Eq. (11):

$$\sigma_{D|IM} = \sqrt{\frac{\sum_1^N (\ln D_i - \mu_{D|IM})^2}{N - 2}} \tag{11}$$
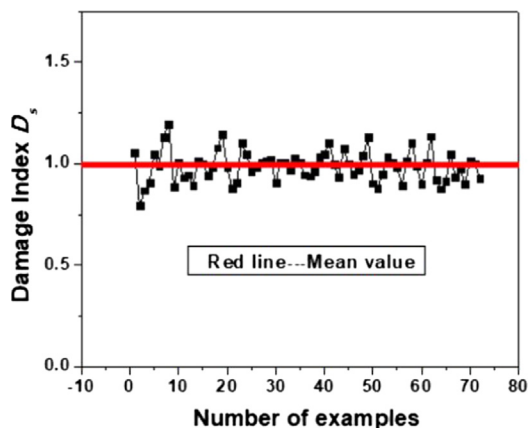
Fig. 5. Accuracy of D_s for aluminum reticulated shells.

The purpose of establishing the PSDM is to determine the median value $\mu_{D|IM}$ and the logarithmic standard deviation $\sigma_{D|IM}$ of the structural seismic demand, which are obtained by the regression study of the data pair of structural response and seismic intensity.

4.3. Probabilistic seismic demand model with uncertainty consideration

Reasonable sampling method can not only reduce the estimation variance of simulation results and improve the simulation accuracy, but also obtain satisfactory results in the case of small samples. Latin Hypercube Sampling (LHS) [31], a widely used sampling method, is adopted in this paper. The basic idea is to stratify the sampling space of input parameters and obtain the input variable values from each layer independently rather than from the whole distribution. Using LHS to generate n samples, it is required to divide each input variable into m equal probability intervals, and randomly extract a value from each interval according to the probability distribution. Since each input distribution has a sample with n values, the LHS sampling is more uniform than the normal random sampling. Samples from each input variable representing mean, variance and other parameters will be more accurate than non-stratified random sampling results. The results show that the sampling times of LHS method are usually 20–40% less than that of simple random sampling method under the same precision requirement.

Probabilistic seismic demand analysis is an important process of transmission of ground motion uncertainty and structural uncertainty. Probabilistic seismic demand analysis can be conducted with the consideration of the uncertainty in the following steps: (1) 40 earthquake motions in Appendix A were selected to consider the uncertainty of the ground motion, σ_{RTR} represented the discreteness of the structural responses caused by ground motion uncertainty; (2) five main structural random parameters are determined to generate structural samples with the consideration of structural uncertainty, σ_M represent the discreteness of the structural responses caused by structural uncertainty; (3) the LHS method is utilized to generate 40 pairs of seismic-structural samples according to the five main random structural parameters in order to consider the randomness and uncertainty of ground motion and structure parameters in this paper. σ_D represented the total discreteness of the structural response caused by the uncertainty of ground motion and structure parameters. The influence of the uncertainty of ground motion and structure parameters on the seismic response of the latticed shells can be obtained by the incremental dynamic analysis.

The value of σ_D can be obtained from Eq. (12):

$$\sigma_D = \sqrt{\sigma_{RTR}^2 + \sigma_M^2} \tag{12}$$

where σ_{RTR} and σ_M represent the dispersion of the structural responses caused by ground motion and structural uncertainties, respectively.

The IDAs are performed on different cylindrical latticed shells with various rise-to-span ratios and roof weights with an input of 40 far-field ground motion records. Three models (C2031806, C2031812 and C2031818) are used as case studies to assess the effects of varied degrees of uncertainty on the PSDM. Two different combinations of uncertainties are considered: (1) only ground motion uncertainty and (2) both ground motion uncertainty and structural uncertainty. Figs. 6 and 7 illustrate the PSDM with consideration of different uncertainties. Fig. 6 shows that when earthquake uncertainty is taken into account individually, the total dispersion of the structural response σ_D of the three models is 0.233, 0.243 and 0.307, respectively. When both earthquake uncertainty and structural uncertainty are considered, the value of σ_D in the three models is 0.276, 0.295 and 0.341, respectively, as shown in Fig. 7. The value of σ_M can be obtained from Eq. (12), which is 0.187, 0.138 and 0.082 for the three models, respectively. Compared with the
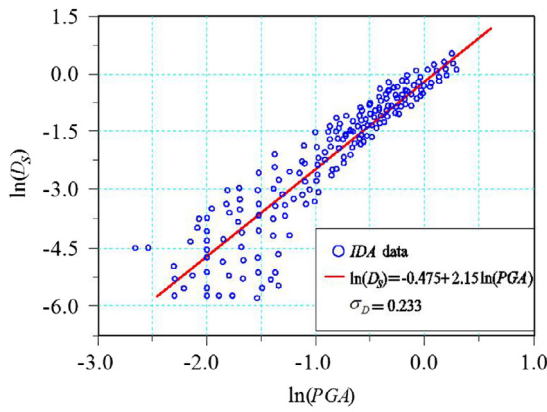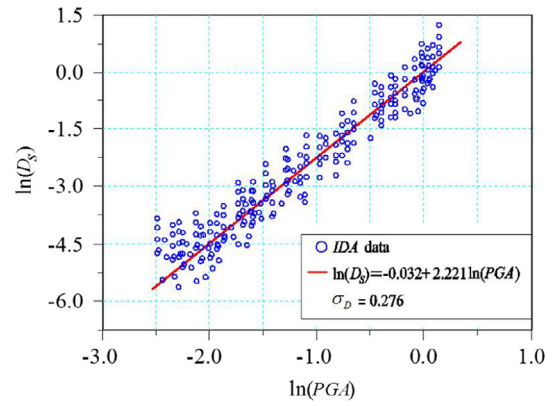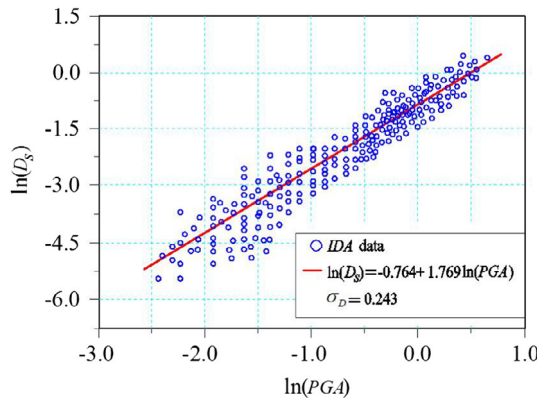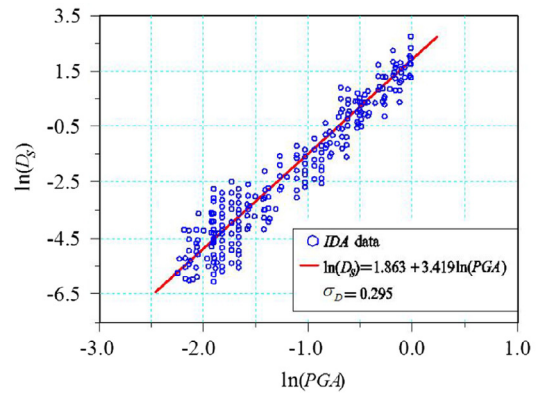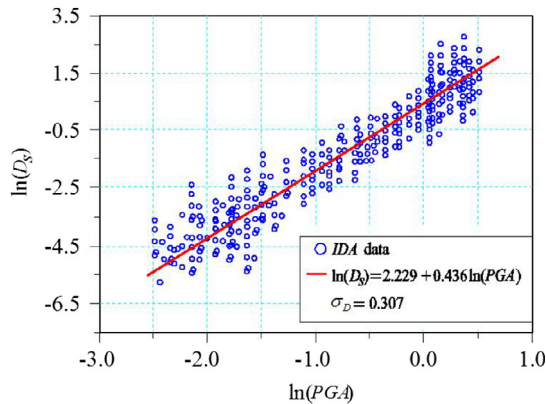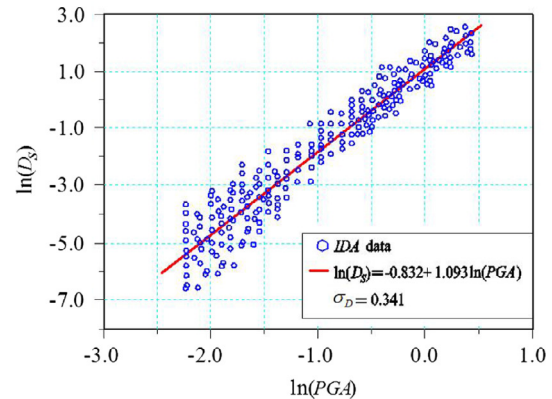
Fig. 6. PSDMs of the cylindrical shells with the consideration of ground motion uncertainty only.

Fig. 7. PSDMs of the cylindrical shells with the consideration of both ground motion uncertainty and structural modelling uncertainty.

structural variability caused by the uncertainty of the earthquake, the structural variability caused by the structural uncertainties cannot be neglected. This has significant influence on the seismic response of the structures and affects the systematic vulnerability. Therefore, the seismic vulnerability analysis of the aluminium alloy latticed shells must consider the effects of structural uncertainties. In addition, the value of $\sigma_M \backslash *$ MERGEFORMAT decreases as the rise-span ratio decreases. The failure mode of the cylindrical reticulated shells with a high rise-span ratio is mainly the dynamic strength failure, which is affected by random factors, such as yield strength (proof stress) and strain. Additionally, the failure mode of the cylindrical reticulated shells with low rise-span ratios is mainly dynamic instability, which is slightly affected by the randomness of material parameters.

4.4. Probabilistic seismic demand model of different reticulated shells

To study the effects of the rise-span ratio and roof loading on the regression parameters, a large-scale parametric analysis is conducted on the cylindrical reticulated shells with an input of 40 far-fault ground motion records and with the consideration of randomness in different parameters, such as the proof stress, the viscous damping ratio and the dead and live loadings. Based on the regression statistics, the PSDMs of the cylindrical latticed shells with varied structural parameters are established, as shown in Table 2. The value of $\beta_0 \backslash *$ MERGEFORMAT increases as the rise-span ratio and roof mass increase, which means that latticed shells with a large rise-span ratio and roof mass are damaged more severely.

Table 2
PSDMs of cylindrical latticed shells with various rise-span ratios and roof masses.

Numbering of models	$\mu_D = \beta_0 + \beta_1 \ln PGA$		σ_D* MERGEFORMAT
	β_0* MERGEFORMAT	β_1* MERGEFORMAT	
C2021806	-0.874	0.964	0.276
C2021812	-0.811	0.952	0.291
C2021818	-0.677	0.936	0.322
C2031806	-1.089	0.972	0.273
C2031812	-0.853	0.958	0.288
C2031818	-0.784	0.946	0.317
C2051806	-1.152	1.008	0.281
C2051812	-1.011	0.989	0.292
C2051818	-0.913	0.978	0.316

5. Probabilistic seismic capacity analysis

5.1. Probabilistic seismic capacity model

Similar to the seismic demand, the seismic capacity of structure C is assumed to follow a lognormal probability distribution. The PSCM is described by Eq. (13):

$$P[D \geqslant C|D = d] = \Phi\left[\frac{\ln d - \ln \mu_c}{\sigma_C}\right]$$
(13)

where μ_c* MERGEFORMAT is the median value of the structural limit state in Eq. (14) and σ_C* MERGEFORMAT is the corresponding logarithmic standard deviation in Eq. (15):

$$\mu_c = \frac{m_c}{\sqrt{1 + \delta_c^2}}$$
(14)

$$\sigma_c = \sqrt{\ln(1 + \delta_c^2)}$$
(15)

where m_c* MERGEFORMAT and δ_C* MERGEFORMAT are the average values of the structural capacity and variation coefficient of different limit states, respectively.

5.2. Structural performance levels

Performance-based seismic design enables designed buildings to meet various predetermined functions or performance objectives during their use. It is necessary for researchers and engineers to establish the structural performance levels of such performance objectives, which can be defined by acceptable levels of damage. Five structural performance levels are considered and determined: (1) insignificant damage, (2) minor damage (*LS1*), (3) moderate damage (*LS2*), (4) severe damage (*LS3*) and (5) collapse (*LS4*).

In order to make the statistical results more accurate, the damage index D_s of 328 single-layer cylindrical reticulated shell examples can be finally obtained by eliminating the examples that can not be distinguished between the adjacent limit states in the statistical analysis of the results. Then, the average values of the structural capacity m_c* MERGEFORMATand variation coefficient δ_C* MERGEFORMATof different limit states can be calculated by the results. Therefore, the statistical results of μ_c* MERGEFORMAT and σ_C* MERGEFORMAT in

Table 3
Statistical results of the damage index D_s with respect to the different levels of damage states of the aluminium alloy reticulated shells.

PSCM	LS1	LS2	LS3	LS4
μ_c* MERGEFORMAT	0.1884	0.3868	0.6903	1.0487
σ_C* MERGEFORMAT	0.3174	0.3014	0.2985	0.3206

Table 3 can be determined by Eqs. (14) and (15). Based on the statistical analysis of the IDA results, the damage index D_s of the performance levels can be obtained according to the discrimination criterion shown in Table 4.

Fig. 8 illustrates the plastic development and damage levels of the aluminium alloy latticed shell (C2051812) with respect to D_s for the IDA. The yielded members are indicated by circles, whose diameters represent the level of plasticity development.

6. Probabilistic seismic fragility analysis

Seismic vulnerability analysis can predict the probability of failure at all levels under different earthquake levels. For seismic loading, the vulnerabilities indicate the probability that the seismic demand (*D*) placed on the structure is greater than the capacity (*C*) of the structure. This probability is conditioned on a chosen intensity measure (*IM*), which represents the degree of seismic loading.

One method of assessing the vulnerability function $F_R(im)$* MERGEFORMAT is developing a probability distribution for the demand conditioned on the *IM*, also known as a PSDM, and convolving it with a distribution for the PSCM. The generic representation of this conditional probability is given by Eq. (16):

$$F_R(im) = P_f[D > C|IM = im] = 1 - \Phi\left[\frac{\ln \mu_c - \ln \mu_{D|IM}}{\sqrt{\sigma_{D|IM}^2 + \sigma_C^2}}\right]$$
(16)

where μ_c* MERGEFORMAT is the median value of the structural capacity; $\mu_{D|IM}$* MERGEFORMAT is the median value of the seismic demand; $\sigma_{D|IM}$* MERGEFORMAT is the associated logarithmic standard deviation of the demand; and σ_C* MERGEFORMAT is the associated logarithmic standard deviation of structural capacity.

Figs. 9 and 10 illustrate the fragility curves for an example aluminium alloy cylindrical reticulated shell with a length of 36 m, width of 20 m, roof load of $120 \, \text{kg/m}^2$ and rise-span ratio of 1/5 under 40 seismic records for different performance levels of *LS1*, *LS2*, *LS3* and *LS4*. The results can be used for the seismic performance evaluation and risk assessment of aluminium alloy cylindrical reticulated shells.

7. Conclusions

A probabilistic seismic vulnerability analysis of aluminium alloy reticulated shells with consideration of uncertainty is performed to evaluate the seismic performance and conduct the risk assessment. The primary findings can be summarized as follows.

(1) A seismic and structural uncertainty analysis is performed. Forty far-fault ground motion records are selected to assess the uncertainty of earthquakes. The probability distributions of 11 structural uncertainties are determined.
(2) The results of the sensitivity analysis illustrate that the proof stress $\sigma_{0.2}$* MERGEFORMAT, viscous damping ratio ξ* MERGEFORMAT, dead load *DL* and live load *LL* are the top four most influential parameters on seismic responses.
(3) The IDA method is applied to carry out the PSDA. A damage index based on the structural responses is proposed to describe the damage levels of the structural member and reticulated shells.
(4) Probabilistic seismic demand models considering the uncertainties are established. The results show that the structural variability caused by structural uncertainties cannot be neglected, which largely affects the seismic responses of the structures and the systematic vulnerability. The PSDAs of different structures show that reticulated shells with a larger rise-span ratio and roof mass have a higher failure probability and more severe damage.
(5) A probabilistic seismic capacity analysis is undertaken and structural damage levels are proposed. According to the statistical results of the damage index D_s with respect to the different levels of the

Table 4
Proposed structural performance levels for aluminium alloy cylindrical reticulated shells.

Damage state	Description	Rule for reticulated shells	D_s
Insignificant	No visible structural or non-structural damage.	No plastic deformation of elements.	0–0.2
Minor (LS1)	Some of the members have yielded, but the plastic development of the member is not deep. No structural repair required.	Before 5P yielded members appear, the structure has no deep damage and no structural repair required.	0.2–0.4
Moderate (LS2)	The yielding of the member is serious, but there is no fracture of the member and the structure maintains its original stiffness. Repairable structural damage has occurred.	Before the full section(8P) yielded member appears, the structure retains its original stiffness and integrity.	0.4–0.7
Severe (LS3)	The plastic development of the member is serious, the rigidity of the structure is sharply weakened, the members are broken and the displacement of the structure increases sharply.	The member enters the entire section yielding, a partial member fails, the structural rigidity weakens sharply and the displacement increases sharply.	0.7–1.0
Collapse (LS4)	Partial or complete collapse of the structure.	Entire collapse of the structure.	1.0

a) D_s=0.2015 b) D_s=0.4134 c) D_s=0.7083 d) D_s=1.0287
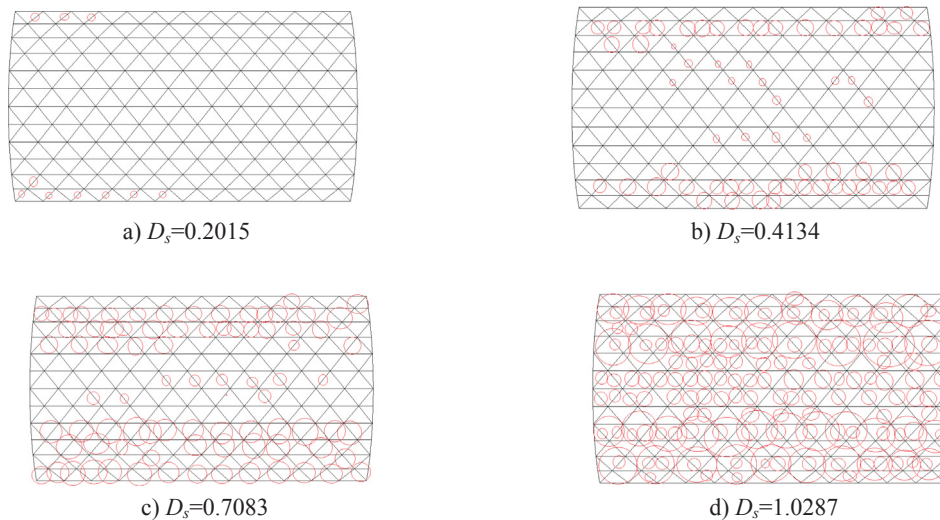
Fig. 8. Damage levels with respect to D_s of the aluminium alloy cylindrical reticulated shells (NGA721).
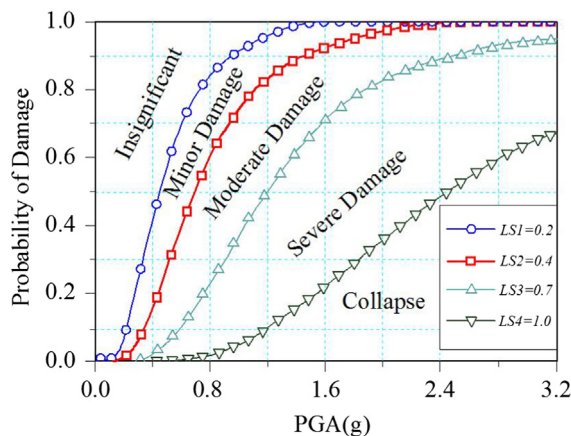
Fig. 9. Fragility curves for performance levels.
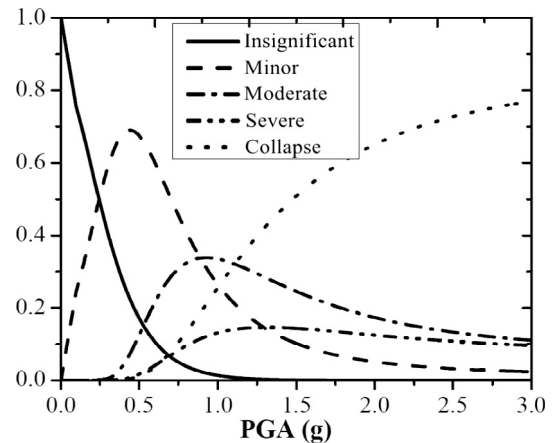
Fig. 10. Probability curves for different damage states.

damage states of the aluminium alloy reticulated shells, the median value of the different structural limit states *LS1*, *LS2*, *LS3* and *LS4* are 0.2, 0.4, 0.7 and 1.0, respectively.
(6) The vulnerability analysis of different levels of structural damage based on a structural damage model is carried out based on the IDAs, which are utilized to predict the failure probability and evaluate the structural performance of aluminium alloy cylindrical latticed shells under different earthquake levels.

Appendix A

40 Selected ground motion records

Earthquake	Number	Moment magnitude	Focal mechanism	Epicentral distance	Site condition	PGA(g)
San Fernando	68	6.61	Reverse	22.77	D	0.2101
Imperial Valley-06	163	6.53	Strike-Slip	24.60	D	0.1033
Imperial Valley-06	167	6.53	Strike-Slip	15.30	D	0.1597
Victoria, Mexico	266	6.33	Strike-Slip	18.96	D	0.1179
Westmorland	316	5.90	Strike-Slip	16.66	D	0.2193
Coalinga-01	322	6.36	Reverse	24.02	D	0.2806
Coalinga-01	323	6.36	Reverse	55.77	C	0.0445
Coalinga-01	324	6.36	Reverse	43.68	D	0.0950
Coalinga-01	327	6.36	Reverse	40.98	C	0.0491
Coalinga-01	331	6.36	Reverse	48.70	D	0.1364
Coalinga-01	334	6.36	Reverse	41.99	D	0.1431
Coalinga-01	336	6.36	Reverse	28.52	C	0.0938
Coalinga-01	342	6.36	Reverse	37.22	C	0.1521
Morgan Hill	449	6.19	Strike-Slip	39.08	D	0.1175
N. Palm Springs	535	6.06	Reverse-Oblique	30.97	D	0.0569
Superstition Hills-02	721	6.54	Strike-Slip	18.20	D	0.2933
Loma Prieta	776	6.93	Reverse-Oblique	27.93	C	0.2794
Loma Prieta	778	6.93	Reverse-Oblique	24.82	D	0.2635
Loma Prieta	787	6.93	Reverse-Oblique	30.86	C	0.2281
Loma Prieta	800	6.93	Reverse-Oblique	32.78	D	0.0959
Cape Mendocino	826	7.01	Reverse	41.97	D	0.1668
Landers	838	7.28	Strike-Slip	34.86	C	0.1193
Landers	900	7.28	Strike-Slip	23.62	D	0.2234
Northridge-01	951	6.69	Reverse	44.11	D	0.0792
Northridge-01	964	6.69	Reverse	47.04	D	0.1058
Northridge-01	966	6.69	Reverse	53.45	D	0.0935
Northridge-01	993	6.69	Reverse	27.26	C	0.2071
Northridge-01	995	6.69	Reverse	24.03	D	0.3354
Northridge-01	1000	6.69	Reverse	31.33	D	0.1412
Northridge-01	1019	6.69	Reverse	35.81	C	0.0796
Northridge-01	1028	6.69	Reverse	37.24	C	0.0771
Northridge-01	1053	6.69	Reverse	41.67	C	0.0676
Northridge-01	1088	6.69	Reverse	57.20	D	0.1583
Northridge-01	1094	6.69	Reverse	51.71	D	0.0636
Kobe, Japan	1116	6.90	Strike-Slip	19.15	D	0.2293
Kocaeli, Turkey	1148	7.51	Strike-Slip	13.49	C	0.1741
Hector Mine	1762	7.13	Strike-Slip	43.05	D	0.1935
Hector Mine	1776	7.13	Strike-Slip	56.40	D	0.0743
Hector Mine	1785	7.13	Strike-Slip	54.68	D	0.0938
Hector Mine	1794	7.13	Strike-Slip	31.06	C	0.1498

References

[1] Wang YJ, Fan F, Lin S. Experimental investigation on the stability of aluminium alloy 6082 circular tubes in axial compression. Thin-Walled Struct 2015;89:54–66.
[2] Mazzolani FM. 3D aluminium structures. Thin-Walled Struct 2012;61:258–66.
[3] Ju QW, Zhu LJ. An introduction to aluminium alloy dome roof structure of Shanghai International Gymnastic Center. J Build Struct 1998;19(3):33–40.
[4] European Committee for Standardization (CEN). Eurocode9: Design of Aluminium Structures, Part 1–1: General Structural Rules. Brussels: CEN; 2007.
[5] Xiong Z, Guo XN, Luo YF, Zhu S. Elasto-plastic stability of single-layer reticulated shells with aluminium alloy gusset joints. Thin-Walled Struct 2017;115:163–75.
[6] Atagi T, Ishikawa K, Okubo S, Hiyama Y. Dynamic behavior of aluminum alloy double layer lean-to roof structure. Annual Meeting Architect Inst Japan 2000:919–20.
[7] Ishikawa K, Okubo S, Hiyama Y. Behavior of aluminum alloy double layer latticed grid roof system supported by two latticed walls : Part 1. horizontal load capacity of the walls. Annual Meeting Architect Inst Japan 2000:929–30.
[8] Ishikawa K, Okubo S. Hiyama Y, Behavior of aluminum alloy double layer latticed grid roof system supported by two latticed walls : Part 2. study on collapse acce-laration of the structure. Annual Meeting Architect Inst Japan 2000:931–2.
[9] Hiyama Y, Ishikawa K, Kato S, Okubo S. Experiments and analysis of the post-buckling behaviors of aluminum alloy double layer space grids applying ball joints. Struct Eng Mech 2000;9(3):289–304.
[10] Xie ZH, Li LJ. Earthquake resistant capability analysis of aluminium alloy double-layer reticulated shell structure. J South China University Technol 2003;31:127–9.
[11] Ma YY, Ma HH, Fan F, Yu ZW. Experimental and theoretical analysis on static be-havior of bolt-column joint under in-plane direction bending in single-layer re-ticulate shells. Thin-Walled Struct 2019;135:472–85.
[12] Guo XN, Liang SP, Shen ZY. Experiment on aluminum alloy members under axial compression. Front Struct Civ Eng 2015;9(1):48–64.
[13] Kissell JR, Ferry RL. Aluminum structures:a guide to their specifications and design. New York: John Wiley&Sons; 2002.
[14] Mazzolani FM. Aluminium alloy structures. 2nd ed. London: Chapman&Hall; 1995.
[15] Adeoti GO, Fan F, Wang Y, Zhai X. Stability of 6082–T6 aluminium alloy columns with H-section and rectangular hollow sections. Thin-Walled Struct 2015;89:1–16.
[16] De Martino A, Landolfo R, Mazzolani FM. The use of the Ramberg-Osgood law for materials of round-house type. Mater Struct 1990;23:59–67.
[17] Padgett JE, DesRoches R. Sensitivity of seismic response and fragility to parameter uncertainty. J Struct Eng 2007;133(12):1710–8.
[18] Joint Committee on Structural Safety. Probabilistic model code. Internet publica-tion; 2001. < http://www.jcss.eth.ch > .
[19] Porter KA, Beck JL, Shaikhutdinov RV. Investigation of sensitivity of building loss estimates to major uncertain variables for the van nuys testbed. California Institute of Technology[R]. PEER Report 2002/2003, Pacific Earthquake Engineering. Berkeley, CA, USA: Research Center, University of California; 2002.
[20] Dolsek M. Incremental dynamic analysis with consideration of modeling un-certainties. Earthq Eng Struct D 2008;38(6):805–25.
[21] Chen GB, Zhang H, Rasmussen Jr K, et al. Modelling geometric imperfections of spatial latticed structures considering correlations of node imperfections. Appl Mech Mater 2014;553:576–81.
[22] Fan F, Yan J, Cao Z. Elasto-plastic stability of single-layer reticulated domes with initial curvature of members. Thin-Walled Struct 2012;60:239–46.
[23] Xie L, Ma Y. Research on performance-based seismic design criteria. Acta Seismol Sin 2002;15(2):214–25.
[24] Rodriguez ME, Aristizabal JC. Evaluation of a seismic damage parameter. Earthq Eng Struct D 1999;28:463–77.
[25] Wong KKF, Wang Y. Energy-based damage assessment on structured during earthquakes. The Struct Des Tall Build 2001;10:135–54.
[26] Park YJ, Ang AHS. Mechanistic seismic damage models for reinforced concrete. J Struct Eng 1985;111(4):722–39.
[27] Yu ZW, Zhi XD, Fan F, Lu C. Effect of substructures upon failure behavior of steel

reticulated domes subjected to the severe earthquake. Thin-Walled Struct 2011;49(9):1160–70.

[28] Cornell CA, Jalayer F, Hamburger RO, et al. The probabilistic basis for the 2000 SAC/FEMA steel moment frame guidelines. J Struct Eng 2002;128(4):526–33.

[29] Ellingwood RR, Celik OC, Kinali K. Fragility assessment of building structural systems in Mid-America. Earthq Eng Struct D 2007;36(13):1935–52.

[30] Nielson BG, DesRoches R. Analytical seismic fragility curves for typical bridges in the central and southeastern United States. Earthq Spectra 2007;23(3):615–33.

[31] Helton JC, Davis FJ. Latin hypercube sampling and the propagation of uncertainty in analyses of complex systems. Reliab Eng Stst Safe 2003;81:23–69.